Altered Hydrogen Bonding of Arg82 during the Proton Pump Cycle of Bacteriorhodopsin: A Low-Temperature Polarized FTIR Spectroscopic Study†

Taro Tanimoto,‡ Mikihiro Shibata,‡ Marina Belenky,§ Judith Herzfeld,§ and Hideki Kandori*,‡

Department of Materials Science and Engineering, Nagoya Institute of Technology, Showa-ku, Nagoya 466-8555, Japan, and Department of Chemistry, Brandeis University, Waltham, Massachusetts 02454-9110

Received March 31, 2004; Revised Manuscript Received May 12, 2004

ABSTRACT: Light-driven proton transport in bacteriorhodopsin (BR) is achieved by dynamic rearrangement of the hydrogen-bonding network inside the membrane protein. Arg82 is located between the Schiff base region and proton release group, and has a major influence on the pK_a values of these groups. It is believed that Arg82 changes its hydrogen-bonding acceptors during the pump cycle of BR, stages of which are correlated with proton movement along the transport pathway. In this study, we compare low-temperature polarized FTIR spectra of [$\eta_{1,2}$-^{15}N]arginine-labeled BR in the 2750−2000 cm^{-1} region with those of unlabeled BR for the K, L, M, and N intermediates. In the K-minus-BR difference spectra, ^{15}N-shifted modes were found at 2292 (−)/2266 (+) cm^{-1} and at 2579 (−)/2567 (+) cm^{-1}. The former corresponds to strong hydrogen bonding, while the latter corresponds to very weak hydrogen bonding. Both N−D stretches probably originate from Arg82, the former oriented toward water 406 and the latter toward the extracellular side, and both hydrogen bonds are somewhat strengthened upon retinal photoisomerization. This perturbation of arginine hydrogen bonding is entirely relaxed in the L intermediate where no ^{15}N-isotope shifts are observed in the difference spectrum. In the M intermediate, the frequency is not significantly altered from that in BR. However, the polarized FTIR spectra strongly suggest that the dipolar orientation of the strongly hydrogen bonded N−D group of Arg82 is changed from perpendicular to parallel to the membrane plane. Such a change is presumably related to the motion of the Arg82 side chain from the Schiff base region to the extracellular proton release group. Additional bands corresponding to weak hydrogen bonding were observed in both the M-minus-BR and N-minus-BR spectra. Changes in hydrogen-bonding structures involving Arg82 are discussed on the basis of these FTIR observations.

Bacteriorhodopsin (BR),[1] a membrane protein found in *Halobacterium salinarum*, functions as a light-driven proton pump with a retinylidene chromophore (*1*, *2*). Absorption of light by the all-trans form of the chromophore triggers a cyclic reaction that comprises a series of intermediates, designated as the J, K, L, M, N, and O states. From the cytoplasmic side to the extracellular side, the proton transport pathway includes Asp96, the Schiff base between retinal and Lys216, Asp85, and the Glu204−Glu194 region. Active transport is achieved by a sequence of proton transfers which must be well-controlled spatially and temporally.

The protonated Schiff base has a diffuse counterion (*3*), the most proximal part of which comprises a roughly planar pentagonal hydrogen-bonded cluster of three water molecules and one oxygen each of Asp85 and Asp212 (*4*, *5*). Changes in the hydrogen bonds of the pentagonal cluster must be related to the primary proton transfer from the Schiff base to Asp85, as well as the subsequent switch in Schiff base connectivity that enforces the vectoriality of the pump (i.e., prevents backflow). On the basis of low-temperature FTIR spectroscopy, we have recently proposed that a hydration switch of a water molecule from Asp85 to Asp212 drives the proton transfer from the Schiff base to Asp85 (*6*). Arg82 forms a hydrogen bond to one of the water molecules in the pentagonal cluster (Figure 1a). Although it is 8 Å away from the Schiff base, the positive charge at Arg82 is probably important in stabilizing the active site in BR by completing an electric quadrupole in this region (*7*, *8*). In fact, Arg82 also plays a crucial role in the correlated pK_a values of Asp85 and Glu204 (*8*−*11*).

After light absorption, photoisomerization of the retinal chromophore leads to formation of the K intermediate. Is this change strictly local, or does it influence the hydrogen bond of Arg82? The subsequent K−L transition involves relaxation of the structure around the retinal chromophore. How does this affect Arg82? Various X-ray structures of the L intermediate differ in this respect, showing either no structural change for Arg82 (*12*, *13*) or movement of the Arg82 side chain toward the proton release group (*14*, *15*). On the other hand, in the M state it is established that the interactions of Arg82 have shifted from the Schiff base region to the extracellular proton release group (Figure 1b) (*16*−*21*). This change is a consequence of the primary proton

† This work was supported by grants from the Japanese Ministry of Education, Culture, Sports, Science, and Technology to H.K. (14380316, 15076202) and by National Institutes of Health Grant EB001035 to J.H.

* To whom correspondence should be addressed. Phone and fax: 81-52-735-5207. E-mail: kandori@nitech.ac.jp.

‡ Nagoya Institute of Technology.

§ Brandeis University.

[1] Abbreviations: BR, bacteriorhodopsin; FTIR, Fourier transform infrared.

10.1021/bi049368p CCC: $27.50 © 2004 American Chemical Society
Published on Web 06/26/2004

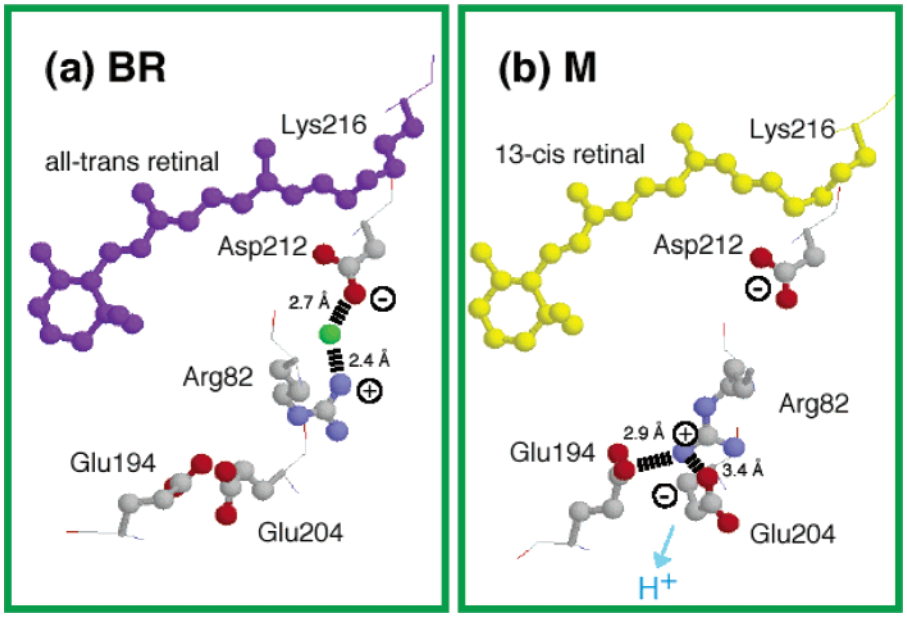

FIGURE 1: X-ray crystallographic structures of the Schiff base region and Arg82 environment in BR (a) and in the M intermediate (b) from PDB entry 1CWQ (*18*). The membrane normal is approximately vertical, and the cytoplasmic and extracellular compartments are above and below, respectively. The green sphere represents the water molecule that bridges Asp212 and Arg82. According to the X-ray structures, Arg82 changes its hydrogen-bonding interaction from the Schiff base region (a) to the extracellular proton release group (b).

transfer from the Schiff base that neutralizes Asp85 and also drives proton release by lowering the pK_a of the surface glutamate complex. Solid-state NMR of [$\eta_{1,2}$-^{15}N]Arg-labeled BR revealed that the environments of the two η-nitrogens of Arg82 are highly asymmetric in the M state (*22*). Perturbation of Arg82 in M has also been reported by FTIR spectroscopy (*23*, *24*). How are these observations related to the structure of the M intermediate? And how does the M−N transition affect the hydrogen bonding of Arg82? In short, our goal is to understand the hydrogen bonding of Arg82 throughout the pump cycle of BR.

Vibrational analysis is a powerful tool for investigating hydrogen bonds (*25*, *26*). In particular, the O−H and N−H stretching modes are good probes. Polarized measurements of oriented BR have the advantage that they can characterize not only the frequencies of vibration, but also their dipolar orientations. In the past, we have applied low-temperature polarized FTIR spectroscopy to oriented BR, and successfully obtained K-minus-BR difference spectra throughout the whole mid-infrared region (4000−700 cm^{-1}) (*27*). Similar spectra of isotope-labeled and mutant BR led to identification of specific vibrational bands. For instance, by using [3-^{18}O]-threonine-labeled BR and mutating individual threonine residues, we revealed the specific interaction of Thr89 with Asp85 in the K, L, and M intermediates (*28*−*30*). In addition, by using [ζ-^{15}N]lysine-labeled BR, we identified the stretching vibration of the Schiff base for BR and the K intermediate (*31*). Analogously, hydration with D_2O and $D_2{}^{18}O$ has allowed the identification of strongly hydrogen bonded water molecules (*32*, *33*) and led to the proposal that altered hydration is involved in the primary proton transfer (*6*).

In the present work, we examine changes in the hydrogen bonding of Arg82 during the pump cycle of BR by means of low-temperature FTIR spectroscopy. To identify the N−D stretching vibrations of arginine in D_2O, we used [$\eta_{1,2}$-^{15}N]-Arg-labeled BR, in which the two terminal nitrogens of the arginine side chains are labeled by ^{15}N (Chart 1). We found

Chart 1

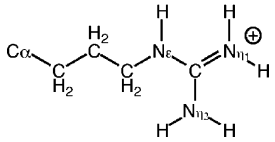

that N−D stretches corresponding to both weak and strong hydrogen bonds change their frequencies in the formation of the K intermediate and both are ascribable to Arg82. In contrast, no arginine bands were identified in the L-minus-BR difference spectra, suggesting that the hydrogen bonds of all the arginine residues in L are identical to those in BR. Thus, it seems that the hydrogen bonding of Arg82 that is altered after light absorption is restored in L. The polarized M-minus-BR spectra indicate that the dipolar orientation of the strongly hydrogen bonded N−D group of Arg82 reorients from perpendicular to parallel to the membrane plane, a change which is presumably related to the movement of the guanidyl group of Arg82 from the Schiff base region to the extracellular proton release group. In addition, N−D stretches at frequencies corresponding to weak hydrogen bonding were observed in difference spectra for both the M and N intermediates. The structure and structural changes of the Arg82 region are discussed in light of these results.

MATERIALS AND METHODS

Previously described methods were used to label BR with [$\eta_{1,2}$-^{15}N]arginine (*22*) and prepare samples for FTIR spectroscopy (*27*, *31*). Preparation of the R82Q mutant protein was also described previously (*23*). The buffers were 2 mM phosphate (pH 7) for the K-minus-BR and L-minus-BR spectra and 2 mM borate (pH 10) for the M-minus-BR and N-minus-BR spectra. A 120 μL aliquot of the sample was dried on a BaF_2 window with a diameter of 18 mm. After hydration by 1 μL of D_2O, the sample was placed in a cell which was then mounted in an Oxford DN-1704 cryostat.

The light-adapted state was obtained by illuminating the film with >500 nm light for 1 min at 273 K.

The details of polarized FTIR spectroscopy are described elsewhere (*27*, *34*). Briefly, a BaF_2 polarizer in the vertical *xy*-plane is placed in front of a mercury−cadmium−technetium (MCT) detector in a Bio-Rad FTS-40 FTIR spectrometer. The IR probe light travels along the *z*-axis to the window with the vertical and horizontal polarizations, A_V and A_H, in the *xz*- and *yz*-planes, respectively. The window in the *xy*-plane was tilted around the vertical *x*-axis by rotating the rod holding the window. The tilt angles (ϕ_0) were 0°, 17.8°, 35.7°, and 53.5°. The dichroic ratio *R* is defined as

$$R = [A_H(\phi_0)/A_H(0°)]/[A_V(\phi_0)/A_V(0°)] \quad (1)$$

Increased intensity of the A_V component due to the increased effective number of BR molecules absorbing light with tilting was corrected in eq 1. *R* is related to the angle of the dipole moment to the membrane normal θ_0 by the previously discussed equation

$$R = 1 + [(\sin^2 \phi_0)/n^2][\rho\langle 9\cos^2\theta_0 - 3\rangle]/[2 - \rho\langle 3\cos^2\theta_0 - 1\rangle] \quad (2)$$

where *n*, the refractive index of the film in the IR region, is assumed to be 1.7 and ρ, the degree of orientation of the membrane, is 0.95 (*27*, *34*). The latter value is revised from the earlier 0.98 on the basis of the observation of an intensity ratio of 1.02 for amide II/amide I in our unhydrated film.

The K-minus-BR spectra were obtained as described previously (*27*). Sixteen independent measurements were averaged with 128 scans for each window tilting angle. The L-minus-BR spectra were obtained according to the method of Maeda et al. (*35*) by which spectra can be accumulated without changing the hydration. Briefly, after the L-minus-BR spectrum was obtained at 170 K, the mixture of BR and L was cooled to 77 K and illuminated sequentially with 501 and >660 nm light before being rewarmed to 170 K. These procedures below 170 K preserve the hydration of the sample, while the photoproducts are reverted to the original BR. Eight independent measurements were averaged with 128 scans for each window tilting angle. The M-minus-BR and N-minus-BR spectra were obtained at 230 and 273 K, respectively, as described previously (*6*). Sixteen independent measurements were averaged with 128 scans for each window tilting angle of the M-minus-BR spectra. Twenty-five independent measurements were averaged with 32 scans for each window tilting angle of the N-minus-BR spectra. From the analysis of the positive 1186 cm^{-1} band that probes the C−C stretch of the protonated 13-*cis*-retinal, present in the N intermediate but not the M intermediate, we estimated the content of the M intermediate to be 30% in the N-minus-BR spectra. The spectral resolution was 2 cm^{-1} for all measurements.

RESULTS

Frequencies and Orientations of the N−D Stretching Vibrations of Arginine in the K-Minus-BR Spectra. Solid and dotted lines in Figure 2 show the K-minus-BR difference spectra in D_2O of the unlabeled and [$\eta_{1,2}$-^{15}N]Arg-labeled BR, respectively, in the N−D stretching region. Positive and negative bands in the two spectra coincide at all window tilting angles except for two peak pairs. The bands at 2579 (−)/2567 (+) cm^{-1} in Figure 2a exhibit a downshift to 2561 (−)/2551 (+) cm^{-1} in the [$\eta_{1,2}$-^{15}N]Arg-labeled BR, indicating that these bands originate from N−D stretches of an arginine side chain. Similarly, the bands at 2292 (−)/2266 (+) cm^{-1} in Figure 2d are assignable to N−D stretches of arginine because of their downward isotope shift. The corresponding N−H stretches of the 2579 (−)/2567 (+) cm^{-1} bands are about 3490 and 3460 cm^{-1}, respectively, while those of the 2292 (−)/2266 (+) cm^{-1} bands are about 3100 and 3000 cm^{-1}, respectively (*27*). Therefore, the 2579 cm^{-1} band in BR corresponds to the N−D stretch for a weak hydrogen bond. On the other hand, the 2292 cm^{-1} band in BR corresponds to the N−D stretch under strongly hydrogen bonding conditions.

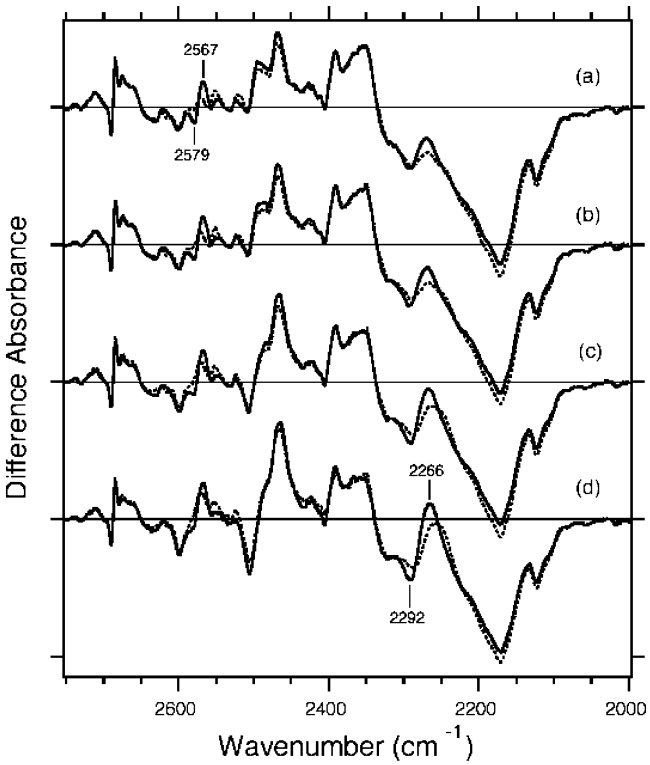

FIGURE 2: K-minus-BR difference infrared spectra of unlabeled (—) and [$\eta_{1,2}$-^{15}N]Arg-labeled (···) BR in the 2750−2000 cm^{-1} region. The sample was hydrated with D_2O, and spectra were measured at 77 K. The window tilting angles are 0° (a), 17.8° (b), 35.7° (c), and 53.5° (d). One division of the *y*-axis corresponds to 0.0015 absorbance unit, and the horizontal straight lines represent zero lines.

It is striking that the dichroic properties of these bands are very different. The shifted 2579 (−)/2567 (+) cm^{-1} bands are clear without the sample being tilted (Figure 2a), while they become less evident as the sample window is tilted (Figure 2b−d). This indicates that the dipole moments of the 2579 (−)/2567 (+) cm^{-1} bands orient along the membrane. We estimated the angle θ of the band at 2579 cm^{-1} to be 80° relative to the membrane normal. Since the positive 2567 cm^{-1} band contains a highly dichroic non-arginine vibration (Figure 2), it was not easy to determine the orientation of this band. By use of the shifted positive band at 2552 cm^{-1} (dotted line in Figure 2), we estimate that the orientation relative to the membrane normal is close

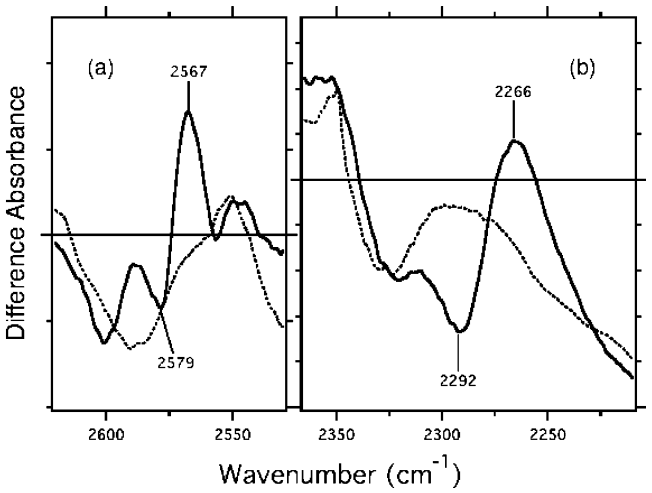

FIGURE 3: K-minus-BR difference infrared spectra of the wild-type (−) and R82Q mutant (···) proteins in the 2620−2530 cm^{-1} (a) and 2365−2210 cm^{-1} (b) regions. The spectra for wild-type BR in (a) and (b) are reproduced from part a and b, respectively, of Figure 2 (solid lines). One division of the *y*-axis corresponds to 0.0002 absorbance unit, and the horizontal straight lines represent zero lines.

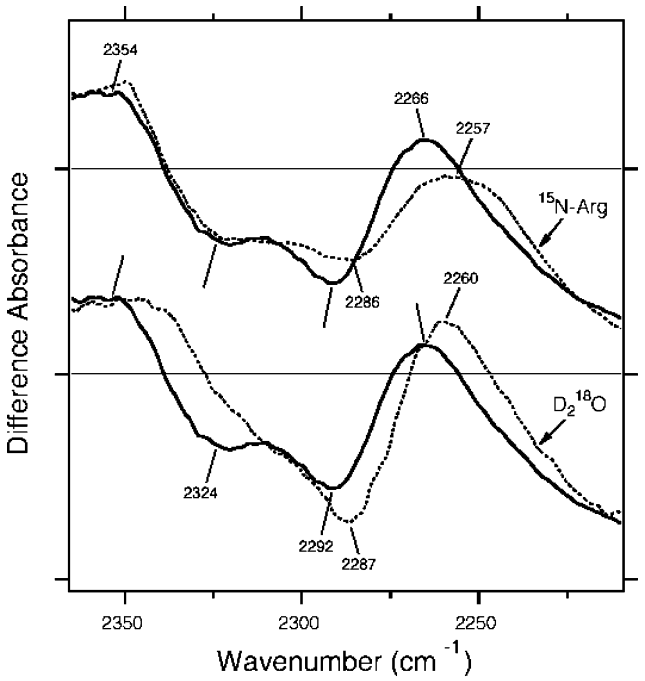

FIGURE 4: K-minus-BR difference infrared spectra in the 2365−2210 cm^{-1} region with the window tilted at 53.5°. The solid traces represent the spectrum of unlabeled BR in D_2O. The upper dotted trace is the spectrum of [$\eta_{1,2}$-^{15}N]Arg-labeled BR in D_2O, while the lower dotted trace is that of unlabeled BR in $D_2{}^{18}O$. One division of the *y*-axis corresponds to 0.0012 absorbance unit, and the horizontal straight lines represent zero lines.

to the magic angle (54.7°). In contrast to the 2579 (−)/2567 (+) cm^{-1} bands, the isotope-shifted 2292 (−)/2266 (+) cm^{-1} bands are more clearly observed when the sample window is tilted, indicating that the corresponding dipole moments are not in the plane of the membrane. The orientations of these dipole moments are discussed further below.

Our observation is that two N−D stretches of arginine side chains are perturbed upon retinal photoisomerization. Which ones might these be? BR has seven arginine residues, each of which has four N−D stretches at the Nη positions in D_2O. However, only Arg82 is embedded inside the membrane. All the other arginines are located at the membrane surface, and even the nearest side chain atoms are >16 Å from the Schiff base nitrogen. Since K formation takes place at 77 K and the absence of global structural change is confirmed by its X-ray structure (*36*−*38*), we consider it safe to assume that differences in the N−D stretches of arginine originate from Arg82. Indeed, Figure 3 shows that the K-minus-BR spectrum of the R82Q mutant protein lacks these bands.

Of the two difference bands, the peak pair at 2292 and 2266 cm^{-1} is of particular interest because previous comparison of spectra in D_2O and $D_2{}^{18}O$ indicated that bands in this region originate from water O−D stretching vibrations (*32*). Figure 4 compares the K-minus-BR difference spectrum of unlabeled BR in D_2O with those of [$\eta_{1,2}$-^{15}N]Arg-labeled BR in D_2O (upper trace) and unlabeled BR in $D_2{}^{18}O$ (lower trace). In $D_2{}^{18}O$, all vibrational bands in this frequency region are shifted. Thus, we previously concluded that the peaks at 2354 (+), 2324 (−), 2292 (−), and 2266 (+) cm^{-1} originate from O−D stretches of water molecules (*32*, *33*). In contrast, only the peaks at 2292 (−) and 2266 (+) cm^{-1} exhibit the ^{15}N-induced shifts of arginine. This strongly suggests that the 2292 (−)/2266 (+) cm^{-1} bands include the N−D stretch of arginine, in addition to water vibrations.

Since the spectral components are highly mixed, it is not easy to estimate the dipolar orientations of the N−D stretches at 2292 (−)/2266 (+) cm^{-1}. Therefore, we attempted to divide the difference spectra into spectral components of arginine and water by Gaussian curve fitting. As shown in Figure 5b, we used four curves for BR and three curves for the K intermediate in the case of the window tilting angle of 53.5°. The 2292 (−)/2264 (+) cm^{-1} bands (black traces) originate from N−D stretches of arginine, and the others (gray traces) are from water O−D stretches. The solid trace of Figure 5a, composed of the seven traces of Figure 5b, exhibits a reasonable fit to the K-minus-BR difference spectrum of the unlabeled BR in D_2O (dotted trace in Figure 5a). For fitting the K-minus-BR difference spectrum of the [$\eta_{1,2}$-^{15}N]Arg-labeled BR in D_2O or unlabeled BR in $D_2{}^{18}O$ (dotted traces in part c or d, respectively, of Figure 5), the arginine or water bands in Figure 5b (black or gray traces, respectively) were downshifted by 13 and 16 cm^{-1} or 10−15 cm^{-1}, respectively. The reasonable coincidence of the fitting curves with the spectra for the [$\eta_{1,2}$-^{15}N]Arg-labeled BR in D_2O (Figure 5c) and unlabeled BR in $D_2{}^{18}O$ (Figure 5d), as well as for the unlabeled BR in D_2O (Figure 5a), shows that the complex spectra in this frequency region can be attributed to the bands shown in Figure 5b.

Similar spectral reconstructions were carried out for the other window tilting angles, $\phi = 0°$, 17.8°, and 35.7° (data not shown). In the procedure, we did not change the peak frequencies, half widths, or isotope shifts of the Gaussian curve; only the peak height was adjusted for the best fit. By these means, the A_H component in eq 1 was obtained for each window tilting angle, and the dichroic ratio, *R*, was calculated by taking the A_V component into account.

Figure 6 plots the *R* values versus $\sin^2 \phi$ for the vibrational bands in the 2300−2250 cm^{-1} region. The filled triangles and circles represent the N−D stretches of arginine for BR and K, respectively, while the open triangles and circles represent the O−D stretches of water for BR and K, respectively. Whereas we previously reported that the highly

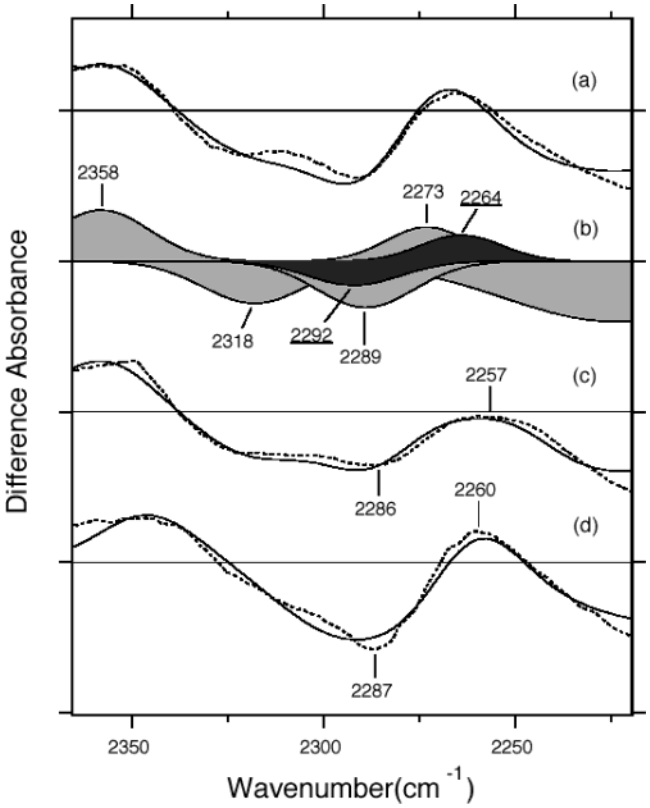

FIGURE 5: Gaussian fits of the K-minus-BR difference spectra in the 2365−2220 cm^{-1} region with the window tilted at 53.5°. One division of the *y*-axis corresponds to 0.0015 absorbance unit, and the horizontal straight lines represent zero lines. (a) Difference spectrum of the unlabeled BR in D_2O (dotted trace) and the fitted curve (solid trace) composed of the Gaussian functions shown in (b). (b) The three positive and four negative bands used to fit the spectra, where the 2292 (−)/2264 (+) cm^{-1} bands (black traces) are regarded as the N−D stretch of arginine. Other bands (gray traces) originate from O−D stretches of water. (c) Difference spectrum of [$\eta_{1,2}$-^{15}N]Arg-labeled BR in D_2O (dotted trace) and the fitted curve (solid trace) using the Gaussian functions with the 2292 (−)/2264 (+) cm^{-1} bands (black traces in (b)) downshifted by 16 and 13 cm^{-1}, respectively. (d) Difference spectrum of unlabeled BR in $D_2{}^{18}O$ (dotted trace) and the fitted curve (solid trace) using the Gaussian functions with water bands (gray traces in b) downshifted as follows: 10 cm^{-1} for the 2358 cm^{-1} band (+), 15 cm^{-1} for the 2318 cm^{-1} band (−), 12 cm^{-1} for the 2289 cm^{-1} band (−), 15 cm^{-1} for the 2273 cm^{-1} band (+), and 12 cm^{-1} for the lowest frequency band at 2221 cm^{-1} (−).

dichroic positive 2266 cm^{-1} band originates from a water O−D stretch (*32*), the present spectra of [$\eta_{1,2}$-^{15}N]Arg-labeled BR clearly show that an arginine N−D stretch also contributes to the band and that both the O−D and N−D stretches are highly dichroic.

All the *R* values increase as the window tilting angle increases, indicating that the angles between the dipole moments and membrane normal are all smaller than the magic angle (54.7°). According to eq 2, the angles of the dipole moments of the arginine N−D stretches in BR (2292 cm^{-1}) and K (2264 cm^{-1}) are determined to be tilted 32° and 25° from the membrane normal, respectively. The former agrees well with the crystallographic values shown in Table 1 (26−34°) for the tilt of the N−O vector between the nitrogen of Arg82 and the oxygen of water 406 relative to the membrane normal in the BR structures (*4*, *5*, *18*, *19*, *36*−*39*). The corresponding N−O distances, being between 2.4 and 2.8 Å (Table 1), are fully consistent with a strong

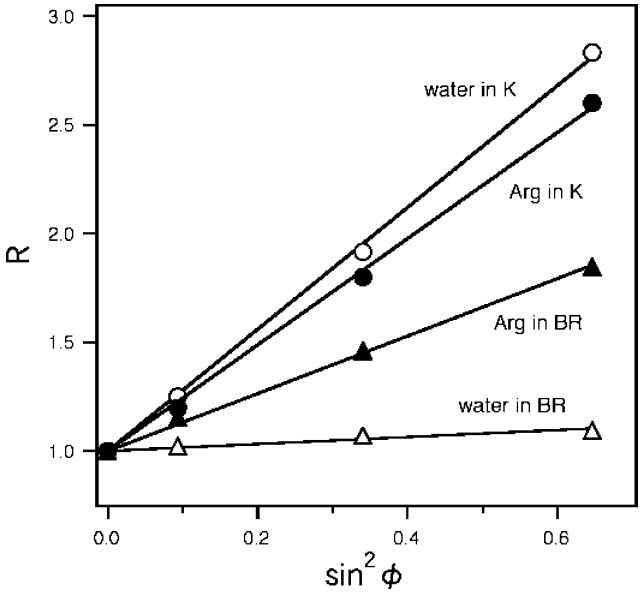

FIGURE 6: *R* versus $\sin^2\phi$ for the arginine N−D stretches at 2264 cm^{-1} (●) and 2292 cm^{-1} (▲) and for the water O−D stretches at 2273 cm^{-1} (○) and 2289 cm^{-1} (△) from the spectral fitting in Figure 5b. The points were fitted with eq 2 by the least-squares method.

Table 1: Structural Data for the Hydrogen Bond between a Terminal Nitrogen of Arg82 and the Oxygen of Water 406 in the BR and K States

		N−O distance (Å)	N−O tilt from the membrane normal (deg)	PDB code (ref)
Luecke et al. (1999)	BR	2.5	33	1C3W (*4*)
Belrhali et al. (1999)	BR	2.6	27	1QHJ (*5*)
Sass et al. (2000)	BR	2.4	28	1CWQ (*18*)
Facciotti et al. (2001)	BR	2.8	34	1KGB (*19*)
Faham et al. (2002)	BR	2.7	a	1KME (*39*)
Edman et al. (2000)	BR	2.7	27	1QKP (*36*)
	K	2.7	26	1QKP (*36*)
Schobert et al. (2002)	BR	2.7	34	1M0L (*37*)
	K	2.9	32	1M0K (*37*)
Matsui et al. (2002)	BR	2.6	31	1IW6 (*38*)
	K	2.6	31	1IXF (*38*)

[a] The membrane normal is not clear in the PDB file.

hydrogen bond. Although there are two other water molecules (water 403 and 407) within hydrogen-bonding distance of the η-nitrogens of Arg82, all the corresponding N−O vectors are tilted by more than the magic angle (54.7°) from the membrane normal. Therefore, the 2292 cm^{-1} N−D stretch can be assigned uniquely to the N−D group of Arg82 that is hydrogen-bonded to water 406, as shown in Figure 1a.

After retinal photoisomerization, the dipole moment of the arginine N−D stretch changes its orientation from 32° to 25° relative to the membrane normal, while the hydrogen bond is strengthened. Whereas the three crystallographic structures of the K intermediate reported very small changes in the length and orientation of the N−O vector (Table 1), the present FTIR study clearly shows the altered hydrogen bonding of the N−D group of Arg82, indicating that retinal isomerization perturbs the hydrogen-bonding network in the water-containing pentagonal cluster structure.

For the O−D stretches of water at 2289 cm^{-1} in BR and 2273 cm^{-1} in K, the dipole moments are determined from eq 2 to be tilted 49° and 23° from the membrane normal,

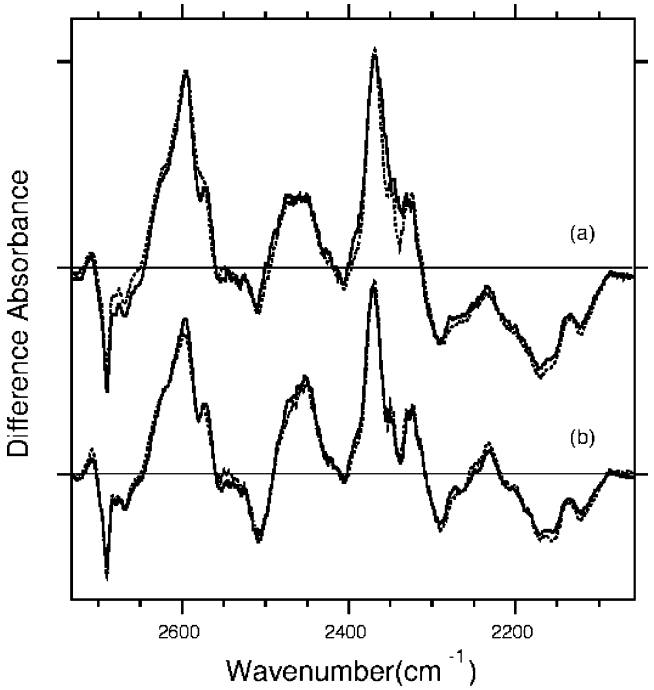

FIGURE 7: L-minus-BR difference infrared spectra of unlabeled (—) and [$\eta_{1,2}$-^{15}N]Arg-labeled (···) BR in the 2730−2060 cm^{-1} region. The sample was hydrated with D_2O, and spectra were measured at 170 K. The window tilting angles are 0° (a) and 53.5° (b). One division of the *y*-axis corresponds to 0.0015 absorbance unit, and the horizontal straight lines represent zero lines.

respectively. In BR crystal structures, the O−O vector between water 406 and Asp212 (Figure 1a) is tilted 48° (PDB code 1CWQ) and 53° (PDB code 1C3W) from the membrane normal. This coincidence suggests the band at 2289 cm^{-1} in BR originates from water 406 bound to Asp212. Mutant studies to further identify these water bands are in progress.

In summary, the K-minus-BR spectra of [$\eta_{1,2}$-^{15}N]Arg-labeled BR show that two N−D stretches of arginine, presumably from Arg82, are perturbed by retinal photoisomerization. The vibrational frequencies indicate that one N−D group is weakly hydrogen bonded (2579 cm^{-1}), whereas the other N−D group is strongly hydrogen bonded (2292 cm^{-1}). Dichroic properties suggest that the latter belongs to the η-nitrogen of Arg82 that is hydrogen bonded to water 406. The shift to lower frequencies in both cases indicates that both hydrogen bonds are strengthened upon retinal photoisomerization.

N−D Stretching Vibrations of Arginine in the L-Minus-BR Spectra. How do hydrogen bonds of Arg82 change in the K−L transition? For strongly hydrogen bonded water, it is known that the perturbations in the K intermediate are relaxed in the L intermediate (*6*). A similar result was obtained for the N−D stretches of arginine. Figure 7 compares the L-minus-BR difference spectra of unlabeled and [$\eta_{1,2}$-^{15}N]Arg-labeled BR at 170 K. Unlike the K-minus-BR spectra, no isotope shift of arginine is evident, indicating that the N−D stretches in L are identical to those in BR. It is particularly noted that the L-minus-BR spectra lack the negative arginine bands at 2579 and 2292 cm^{-1} that are present in the K-minus-BR spectra. Thus, perturbation of Arg82 in the K intermediate is apparently relaxed in the L intermediate.

Several crystallographic structures have been reported for the L intermediate. One group finds that Arg82 moves from

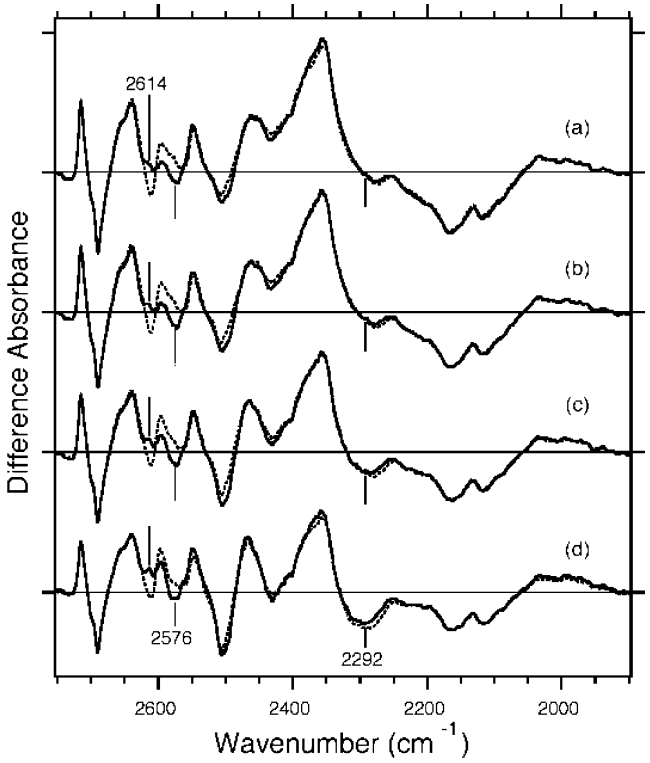

FIGURE 8: M-minus-BR difference infrared spectra of unlabeled (—) and [$\eta_{1,2}$-^{15}N]Arg-labeled (···) BR in the 2750−1900 cm^{-1} region. The sample was hydrated with D_2O, and spectra were measured at 230 K. The window tilting angles are 0° (a), 17.8° (b), 35.7° (c), and 53.5° (d). One division of the *y*-axis corresponds to 0.0012 absorbance unit, and the horizontal straight lines represent zero lines.

the Schiff base region to the extracellular proton release group in the L intermediate (*14*, *15*). In contrast, others find no structural change in the vicinity of Arg82 in the L intermediate (*12*, *13*). Our results strongly support the latter conclusion, since we find no changes in either the frequencies or the dipole orientations for arginine N−D bonds.

N−D Stretching Vibrations of Arginine in the M-Minus-BR Spectra. Figure 8 compares the M-minus-BR difference spectra between unlabeled and [$\eta_{1,2}$-^{15}N]Arg-labeled BR at pH 10 and 230 K. A clear isotope effect is only evident at about 2600 cm^{-1}. The same results were obtained for the sample at pH 7 (data not shown). The negative 2576 cm^{-1} band of the unlabeled BR clearly disappears in the [$\eta_{1,2}$-^{15}N]Arg-labeled BR, indicating that this band contains the N−D stretch of arginine. However, the isotope shift of this band is not characteristic of the ^{14}N/^{15}N shift, since the negative band is observed at higher frequency (about 2614 cm^{-1}) for [$\eta_{1,2}$-^{15}N]Arg-labeled BR (Figure 8). This may be due to the fact that there is no peak at about 2614 cm^{-1} for the unlabeled BR, while a negative peak appears for [$\eta_{1,2}$-^{15}N]Arg-labeled BR in Figure 8a. This suggests the presence of a positive arginine band at 2614 cm^{-1} that cancels the negative band at the same frequency. In fact, there is a positive peak at about 2600 cm^{-1} for [$\eta_{1,2}$-^{15}N]Arg-labeled BR, presumably shifted from 2614 cm^{-1}. On the other hand, it is puzzling that [$\eta_{1,2}$-^{15}N]Arg-labeled BR showed no clear negative band downshifted from 2576 cm^{-1}. Perhaps both the reduction of the negative band and slightly lower frequency shift originate from the isotope effect.

The negative 2576 cm^{-1} band of arginine in the M-minus-BR spectra is close in frequency to the 2579 cm^{-1} band in

Table 2: Structural Data for the Hydrogen-Bonding Possibilities of a Terminal Nitrogen of Arg82 in the M Intermediate

	BR variant	hydrogen bond acceptor	N−O distance (Å)	N−O tilt angle (deg)	PDB code (ref)
Luecke et al. (1999)	D96N	water407	3.1	50	1C8S (*16*)
Luecke et al. (2000)	E204Q	oxygen of Glu194	2.8	30	1F4Z (*17*)
Sass et al. (2000)	wild type	oxygen of Glu204	2.9	75	1CWQ (*18*)
Facciotti et al. (2001)	wild type	oxygen of Glu204	2.7	43	1KG8 (*19*)
		oxygen of Glu194	3.1	84	1KG8 (*19*)
Lanyi et al. (2002)	wild type	water 407[a]	2.7	87[a]	1M0M (*20*)
Schobert et al. (2003)	wild type	water 407[a]	2.8	66[a]	1P8U (*21*)
Takeda et al.	wild type	oxygen of Glu204	2.8	57	1DZE[b]

[a] These structures describe M1, where Arg82 does not move toward the extracellular side. [b] Yet to be published.

the K-minus-BR spectra (Figure 2a), suggesting that the N−D stretch originates from Arg82. This assignment is also consistent with the dipolar orientation. In Figure 7, the intensity of the negative 2576 cm^{-1} band is reduced when the window is tilted, just as observed for the negative 2579 cm^{-1} band in Figure 2. Thus, we infer that a N−D stretch in a weak hydrogen bond of Arg82 is located at 2576−2579 cm^{-1} in BR, downshifted in K (2567 cm^{-1}), restored in L, and upshifted in M (2614 cm^{-1}).

Interestingly, the M-minus-BR spectrum of the untilted sample shows no changes in the 2292 cm^{-1} region where the K-minus-BR spectrum showed perturbation of the N−D stretch of a strong Arg82 hydrogen bond. However, when we tilt the window, reproducible spectral variation accompanying a lower frequency shift is observed at around 2292 cm^{-1} (Figure 8b−d). The deviation in Figure 8d is larger than the present baseline distortion, indicating that the negative band at 2292 cm^{-1} contains a N−D stretching vibration of arginine. From the identity in frequency, the N−D stretch presumably originates from Arg82.

Significantly, no positive peak is observed corresponding to the negative 2292 cm^{-1} band in the tilted samples. However, Figure 6 showed that the intensity of the 2292 cm^{-1} band in BR is 1.85 times larger at 53.5° than at 0°, whereas the observed negative intensity is almost zero at 0° but about 0.00025 absorbance at 53.5°. Thus, it seems that the N−D stretch possesses the same frequency, but different orientations, between BR and the M state. In particular, the present result can best be explained if the dipole moments of the 2292 cm^{-1} band are perpendicular and parallel to the membrane in BR and M, respectively. Thus, the present polarized FTIR spectra suggest that the N−D stretches of Arg82 are similar in frequency (2292 cm^{-1}), but change dipolar orientation between BR and the M intermediate, from 32° to >54.7° relative to the membrane normal. This is consistent with the current understanding that the side chain of Arg82 moves from the Schiff base region to the extracellular proton release group, which possesses a negative charge after the release of a proton.

Table 2 shows the possible hydrogen bond acceptors of Arg82 in the M intermediate according to the crystallographic structures. Compared to those of BR and the K intermediate (Table 1), there are greater variations in the structures of the M intermediate. Nevertheless, other than in the M structure of E204Q, whose proton release group is modified (PDB code 1F4Z (*17*)), the hydrogen bonds between a terminal nitrogen of Arg82 and its acceptor (the N−O vector) are considerably tilted from the membrane normal. In addition, other than in the M1 structures (PDB codes 1M0M (*20*) and 1P8U (*21*)), the hydrogen bond acceptor of Arg82 appears to be the oxygen atom of Glu204 or Glu194 in the negatively charged proton release group in the M intermediate. Thus, the observed dipolar orientation of the N−D stretch of Arg82 corresponding to strong hydrogen bonding is consistent with the crystallographic structures of the late M (M2) intermediate.

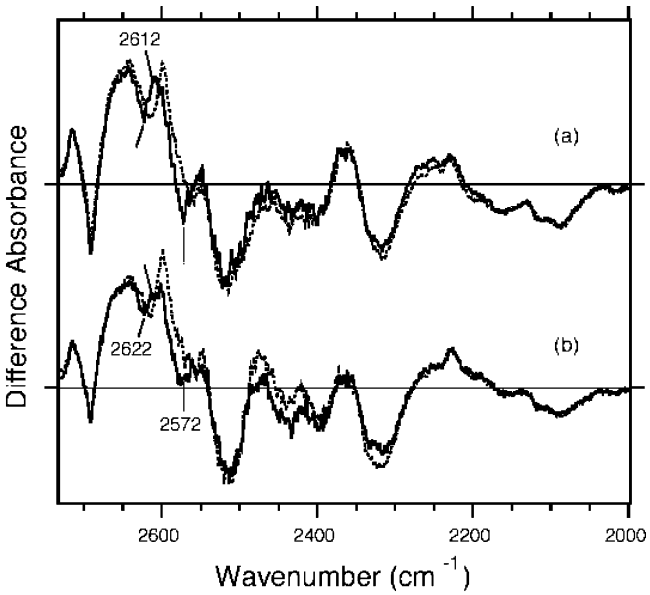

FIGURE 9: N-minus-BR difference infrared spectra of unlabeled (—) and [$\eta_{1,2}$-^{15}N]Arg-labeled (···) BR in the 2730−2000 cm^{-1} region. The sample was hydrated with D_2O, and spectra were measured at 273 K. The window tilting angles are 0° (a) and 53.5° (b). One division of the *y*-axis corresponds to 0.0025 absorbance unit, and the horizontal straight lines represent zero lines.

N−D stretching Vibrations of Arginine in the N-Minus-BR Spectra. Figure 9 compares the N-minus-BR difference spectra for unlabeled and [$\eta_{1,2}$-^{15}N]Arg-labeled BR at 273 K. Although isotope effects are clearly observed at about 2600 cm^{-1}, as in the M-minus-BR spectra (Figure 8), the isotope effect seen at around 2292 cm^{-1} in the M-minus-BR spectra is absent in the N-minus-BR spectra. This suggests that the strongly hydrogen bonded N−D group of Arg82 is somewhat altered in the M-to-N transition. However, since the baseline is much less stable for the measurements of the N-minus-BR spectra, quantitative argument is difficult.

The negative bands at 2622 and 2572 cm^{-1} and the positive band at 2612 cm^{-1} exhibit isotope shifts of ^{15}N-labeled arginine, indicating that these bands contain N−D stretches of arginine. The 2572 cm^{-1} band is close in frequency and dipolar orientation to the 2579 cm^{-1} band in the K-minus-

BR spectra (Figure 2) and the 2576 cm^{-1} band in the M-minus-BR spectra (Figure 8). Thus, we concluded that the 2572 cm^{-1} band originates from Arg82, which shifts to 2612 cm^{-1} upon N formation.

In addition to the 2572 (−)/2612 (+) cm^{-1} bands, a new arginine band appears at 2622 (−) cm^{-1}. The corresponding positive band is probably also located at 2612 cm^{-1}. This arginine band may originate from Arg82. However, Arg134 may also be a candidate, since it is near the extracellular proton release group. It is also possible that an arginine on the cytoplasmic surface contributes to the signal, since N formation involves structural changes in this side of the protein.

DISCUSSION

The present polarized FTIR spectroscopy identifies the frequencies and dipolar orientations of the N−D stretching vibrations of Arg82 in BR and the K, L, M, and N photocycle intermediates. From FTIR difference spectra in these states, we found that three N−D groups of arginine change their hydrogen bonds. Their frequencies in BR are 2292, 2579 (2576 or 2572 cm^{-1}), and 2622 cm^{-1}. Among the bands, the 2292 cm^{-1} band corresponds to a N−D stretch under strongly hydrogen bonding conditions, while the other bands at 2579 and 2622 cm^{-1} correspond to N−D stretches under weakly hydrogen bonding conditions.

It is noted that one arginine side chain possesses five N−D stretches in D_2O (Chart 1). Of these, only the two pairs on the two terminal nitrogens are shifted by the ^{15}N-labeling scheme that we have used. Under homogeneous conditions, the two N−D stretches in each pair are highly coupled and generate symmetric and asymmetric vibrations with similar frequencies. In contrast, if there is a great disparity in the hydrogen bonding of the two deuteriums on one nitrogen, the N−D vibrations are decoupled and appear in different frequency regions. The BR structure in Figure 1a suggests that the latter may be the case. Arg82 and Asp212 form an ion pair through a bridged water molecule. It is likely that this water molecule is highly polarized, and that the hydrogen bond of Arg82 with the water is very strong. We infer that the 2292 cm^{-1} band originates from this N−D stretch of Arg82. This assignment is strongly supported by the fact that the dipolar orientation of the 2292 cm^{-1} band (32°) coincides with the angle between the N−O vector (nitrogen of Arg82 and oxygen of water 406) and the membrane normal in two crystallographic BR structures (Table 1). Previous FTIR spectroscopy revealed that the N−D stretch of the Schiff base (*31*), the O−D stretch of Thr89 (*28*−*30*), and the O−D stretches of water (*6*, *32*, *33*) are very low in frequency, demonstrating a number of strong hydrogen bonds in the Schiff base region. Here we add an additional structural element, the N−D group of Arg82.

In the K intermediate, the strong hydrogen bond (2292 cm^{-1}) is apparently further strengthened as seen from the spectral downshift to 2266 cm^{-1}. Thus, structural changes caused by retinal photoisomerization are extended to Arg82, more than 8 Å away. The strong hydrogen bond of Arg82 is restored to its original strength in the L intermediate. Interaction of Arg82 with a negatively charged Asp212 through water 406 (Figure 1) is likely to persist in the L intermediate. In the M intermediate, the frequency is also not significantly altered from that in BR, although the polarized FTIR spectra strongly suggest that dipolar orientation of the N−D group of Arg82 under strongly hydrogen bonding conditions is changed from perpendicular to parallel to the membrane plane. Such a change is presumably correlated with the molecular motion of Arg82 from the Schiff base region to the extracellular proton release group. The identical vibrational frequency in BR and M, despite different hydrogen bond acceptors, suggests that hydrogen-bonding interactions play a crucial role in stabilizing the protein structure in intermediate states. Since motion of Arg82 away from the Schiff base region presumably destabilizes the negative charge of Asp212, it must be compensated by other elements, including perhaps strong hydration by the water molecule between the Schiff base and Asp85 (*6*).

In addition to the N−D stretch at 2292 cm^{-1}, another N−D stretch at 2579 cm^{-1} that changes its frequency in the K intermediate presumably also originates from Arg82. This weak hydrogen bond is also strengthened upon retinal photoisomerization and restored in the L intermediate, while being weakened in the M and N intermediates. These changes probably probe the local environment of Arg82. The N-minus-BR spectra show another weakly hydrogen bonded N−D band at 2622 (−) cm^{-1}. Since this arginine N−D stretch only changes in the N intermediate, it may originate from arginine at a position other than 82.

In conclusion, we identified N−D stretching vibrations of arginine in D_2O by using [$\eta_{1,2}$-^{15}N]Arg-labeled BR. We found that two N−D stretches of Arg82 change their frequencies in the formation of the K intermediate. In contrast, no arginine bands were identified in the L-minus-BR difference spectra, suggesting that the changes are reversed in L. Perturbations are once again evident in the M-minus-BR and N-minus-BR states. Polarized measurements for the M-minus-BR spectra suggest motion of Arg82 by detecting different dipolar orientations for the vibration at 2292 cm^{-1}. Additional bands were observed in N-minus-BR spectra for N−D vibrations under weakly hydrogen bonding conditions. Further experimental and theoretical efforts including ^{15}N-arginine-labeled BR at different positions will lead to better understanding of the functional role of arginine during the proton pump of BR.

ACKNOWLEDGMENT

We thank Drs. Mark S. Braiman and Yuji Furutani for valuable discussion.

REFERENCES

1. Haupts, U., Tittor, J., and Oesterhelt, D. (1999) Closing in on Bacteriorhodopsin: Progress in Understanding the Molecule, *Annu. Rev. Biopyhs. Biomol. Struct. 28*, 367−399.
2. Lanyi, J. K. (1999) Molecular Mechanism of Ion Transport in Bacteriorhodopsin: Insights from Crystallographic, Spectroscopic, Kinetic, and Mutational Studies, *J. Phys. Chem. B 104* 11441−11448.
3. de Groot, H. J. M., Smith, S. O., Courtin, J., van den Berg, E., Winkel, C., Lugtenburg, J., Griffin, R., and Herzfeld, J. (1990) Solid-State ^{13}C and ^{15}N NMR Study of the Low pH Forms of Bacteriorhodopsin, *Biochemistry 29*, 6873−6883.
4. Luecke, H., Schobert, B., Richter, H.-T., Cartailler, J. P., and Lanyi, J. K. (1999) Structure of Bacteriorhodopsin at 1.55 Å Resolution, *J. Mol. Biol. 291*, 899−911.

5. Belrhali, H., Nollert, P., Royant, A., Menzel, C., Rosenbusch, J., Landau, E. M., and Pebay-Peyroula, E. (1999) Protein, lipid and water organization in bacteriorhodopsin crystals: a molecular view of the purple membrane at 1.9 Å resolution, *Structure 7*, 909−917.
6. Tanimoto, T., Furutani, Y., and Kandori, H. (2003) Structural Changes of Water in the Schiff Base Region of Bacteriorhodopsin: Proposal of a Hydration Switch Model, *Biochemistry 42*, 2300−2306.
7. Stern, L. J., and Khorana, H. G. (1989) Structure−Function Studies on Bacteriorhodopsin: X. Individual Substitutions of Arginine Residues by Glutamine Affect Chromophore Formation, Photocycle, and Proton Translocation, *J. Biol. Chem. 264*, 14202−14208.
8. Balashov, S. P., Govindjee, R., Kono, M., Imasheva, E., Lukashev, E., Ebrey, T. G., Crouch, R. K., Menick, D. R., and Feng, Y. (1993) Effect of the Arginine-82 to Alanine Mutation in Bacteriorodopsin on Dark Adaptation, Proton Release, and the Photochemical Cycle, *Biochemistry 32*, 10331−10343.
9. Balashov, S. P., Govindjee, R., Imasheva, E. S., Misra, S., Ebrey, T. G., Feng, Y., Crouch, R. K., and Menick, D. R. (1995) The Two pKa's of Aspartate-85 and Control of Thermal Isomerization and Proton Release in the Arginine-82 to Lysine Mutant of Bacteriorhodopsin, *Biochemistry 34*, 8820−8834.
10. Richter, H.-T., Brown, L. S., Needleman, R., and Lanyi, J. K. (1996) A Linkage of the pKa's of asp-85 and glu-204 Forms Part of the Reprotonation Switch of Bacteriorhodopsin, *Biochemistry 35*, 4054−4062.
11. Balashov, S. P., Imasheva, E. S., Ebrey, T. G., Chen, N., Menick, D. R., and Crouch, R. K. (1997) Glutamate-194 to Cysteine Mutation Inhibits Fast Light-Induced Proton Release in Bacteriorhodopsin, *Biochemistry 36*, 8671−8676.
12. Lanyi, J. K., and Schobert, B. (2003) Mechanism of Proton Transport in Bacteriorhodopsin from Crystallographic Structures of the K, L, M1, M2, and M2′ Intermediates of the Photocycle, *J. Mol. Biol. 328*, 439−450.
13. Kouyama, T., Nishikawa, T., Tokuhisa, T., and Okumura, H. (2004) Crystal Structure of the L Intermediate of Bacteriorhodopsin: Evidence for Vertical Translocation of a Water Molecule during the Proton Pumping Cycle, *J. Mol. Biol. 335*, 531−546.
14. Royant, A., Edman, K., Ursby, T., Pebay-Peyroula, E., Landau, E. M., and Neutze, R. (2000) Helix Deformation is Coupled to Vertical Proton Transport in the Photocycle of Bacteriorhodopsin, *Nature 406*, 645−648.
15. Edman, K., Royant, A., Larsson, G., Jacobson, F., Taylor, T., Van Der Spoel, D., Landau, E. M., Pebay-Peyroula, E., and Neutze, R. (2004) Deformation of Helix C in the Low Temperature L-Intermediate of Bacteriorhodopsin, *J. Biol. Chem. 279*, 2147−2158.
16. Luecke, H., Schobert, B., Richiter, H. T., Cartailler, J. P., and Lanyi, J. K. (1999) Structural Changes in Bacteriorhodopsin During Ion Transport at 2 Angstrom Resolution, *Science 286*, 255−261.
17. Luecke, H., Schobert, B., Cartailler, J.-P., Richter, H.-T., Rosengarth, A., Needleman, R., and Lanyi, J. K. (2000) Coupling Photoisomerization of the Retinal in Bacteriorhodopsin to Directional Transport, *J. Mol. Biol. 300*, 1237−1255.
18. Sass, H. J., Büldt, G., Gessenich, R., Hehn, D., Neff, D., Schlesinger, R., Berendzen, J., and Ormos, P. (2000) Structural Alterations for Proton Translocation in the M State of Wild-Type Bacteriorhodopsin, *Nature 406*, 649−653.
19. Facciotti, M. T., Rouhani, S., Burkard, F. T., Betancourt, F. M., Downing, K. H., Rose, R. B., McDermott, G., and Glaeser, R. M. (2002) Structure of an Early Intermediate in the M-State Phase of the Bacteriorhodopsin Photocycle, *Biophys. J. 81*, 3442−3455.
20. Lanyi, J. K., and Schobert, B. (2002) Crystallographic Structure of the Retinal and the Protein after Deprotonation of the Schiff Base: The Switch in the Bacteriorhodopsin Photocycle, *J. Mol. Biol. 321*, 727−737.
21. Schobert, B., Brown, L. S., and Lanyi, J. K. (2003) Crystallographic Structures of the M and N Intermediates of Bacteriorhodopsin: Assembly of a Hydrogen-Bonded Chain of Water Molecules between Asp-96 and the Retinal Schiff Base, *J. Mol. Biol. 330*, 553−570.
22. Petkova, A. T., Hu, J. G., Bizounok, M., Simpson, M., Griffin, R. G., and Herzfeld, J. (1999) Arginine Activity in the Proton-Motive Photocycle of Bacteriorhodopsin: Solid-State NMR Studies of the Wild-Type and D85N Proteins, *Biochemistry 38*, 1562−1572.
23. Hatanaka, M., Sasaki, J., Kandori, H., Ebrey, T. G., Needleman, R., Lanyi, J. K., and Maeda, A. (1996) Effects of Arginine-82 on the Interactions of Internal Water Molecules in Bacteriorhodopsin, *Biochemistry 35*, 6308−6312.
24. Hutson, M. S., Alexier, U., Shilov, S. V., Wise, K. J., and Braiman, M. S. (2000) Evidence for a Perturbation of Arginine-82 in the Bacteriorhodopsin Photocycle from Time-Resolved Infrared Spectra, *Biochemistry 39*, 13189−13200.
25. Maeda, A., Kandori, H., Yamazaki, Y., Nishimura, S., Hatanaka, M., Chon, Y.-S., Sasaki, J., Needleman, R., and Lanyi, J. K. (1997) Intramembrane Signaling Mediated by Hydrogen-Bonding of Water and Carboxyl Groups in Bacteriorhodopsin and Rhodopsin, *J. Biochem. 121*, 399−406.
26. Kandori, H. (2000) Role of Internal Water Molecules in Bacteriorhodopsin, *Biochim. Biophys. Acta 1460*, 177−191.
27. Kandori, H., Kinoshita, N., Maeda, A., and Shichida, Y. (1998) Protein Structural Changes in Bacteriorhodopsin upon Photoisomerization As Revealed by Polarized FTIR Spectroscopy, *J. Phys. Chem. B 102*, 7899−7905.
28. Kandori, H., Kinoshita, N., Yamazaki, Y., Maeda, A., Shichida, Y., Needleman, R., Lanyi, J. K., Bizounok, M., Herzfeld, J., Raap, J., and Lugtenburg, J. (1999) Structural Change of Threonine 89 upon Photoisomerization in Bacteriorhodopsin As Revealed by Polarized FTIR Spectroscopy, *Biochemistry 38*, 9676−9683.
29. Kandori, H., Kinoshita, N., Yamazaki, Y., Maeda, A., Shichida, Y., Needleman, R., Lanyi, J. K., Bizounok, M., Herzfeld, J., Raap, J., and Lugtenburg, J. (2000) Local and Distant Protein Structural Changes on Photoisomerization of the Retinal in Bacteriorhodopsin, *Proc. Natl. Acad. Sci. U.S.A. 97*, 4643−4648.
30. Kandori, H., Yamazaki, Y., Shichida, Y., Raap, J., Lugtenburg, J., Belenky, M., and Herzfeld, J. (2001) Tight Asp-85-Thr-89 Association during the Pump Switch of Bacteriorhodopsin, *Proc. Natl. Acad. Sci. U.S.A. 98*, 1571−1576.
31. Kandori, H., Belenky, M., and Herzfeld, J. (2002) Vibrational Frequency and Dipolar Orientation of the Protonated Schiff Base in Bacteriorhodopsin before and after Photoisomerization, *Biochemistry 41*, 6026−6031.
32. Kandori, H., and Shichida, Y. (2000) Direct Observation of the Bridged Water Stretching Vibrations Inside a Protein, *J. Am. Chem. Soc. 122*, 11745−11746.
33. Shibata, M., Tanimoto, T., and Kandori, H. (2003) Water Molecules in the Schiff Base Region of Bacteriorhodopsin, *J. Am. Chem. Soc. 125*, 13312−13313.
34. Hatanaka, M., Kandori, H., and Maeda, A. (1997) Localization and Orientation of Functional Water Molecules in Bacteriorhodopsin as Revealed by Polarized Fourier Transform Infrared Spectroscopy, *Biophys. J. 73*, 1001−1006.
35. Maeda, A., Tomson, F. L., Gennis, R. B., Ebrey, T. G., and Balashov, S. P. (1999) Chromophore-Protein-Water Interactions in the L Intermediate of Bacteriorhodopsin: FTIR Study of the Photoreaction of L at 80 K, *Biochemistry 38*, 8800−8807.
36. Edman, K., Nollert, P., Royant, A., Belrhali, H., Pebey-Peyroula, E., Hajdu, J., Neutze, R., and Landau, E. M. (1999) High-resolution X-ray structure of an early intermediate in the bacteriorhodopsin photocycle, *Nature 401*, 822−826.
37. Schobert, B., Cupp-Vickery, J., Hornak, V., Smith, S. O., and Lanyi, J. K. (2002) Crystallographic Structure of the K Intermediate of Bacteriorhodopsin: Conservation of Free Energy after Photoisomerization of the Retinal, *J. Mol. Biol. 321*, 715−726.
38. Matsui, Y., Sakai, K., Murakami, M., Shiro, Y., Adachi, S., Okumura, H., and Kouyama, T. (2002) Specific Damage Induced by X-ray Radiation and Structural Changes in the Primary Photoreaction of Bacteriorhodopsin, *J. Mol. Biol. 324*, 469−481.
39. Faham, S., and Bowie, J. U. (2002) Bicelle Crystallization: A New Method for Crystallizing Membrane Proteins Yields a Monomeric Bacteriorhodopsin Structure, *J. Mol. Biol. 316*, 1−6.

BI049368P